

ISSN: (Print) (Online) Journal homepage: <https://www.tandfonline.com/loi/gmcl20>

Interaction of hectorite clay with a phospholipid monolayer at air-saline interface in presence of a fluorescent dye

Tanmoy Singha, Ujjal Saren, Pradip Maiti, Utsav Chakraborty, Alapan Pal & Pabitra Kumar Paul

To cite this article: Tanmoy Singha, Ujjal Saren, Pradip Maiti, Utsav Chakraborty, Alapan Pal & Pabitra Kumar Paul (2021): Interaction of hectorite clay with a phospholipid monolayer at air-saline interface in presence of a fluorescent dye, Molecular Crystals and Liquid Crystals, DOI: [10.1080/15421406.2021.2013590](https://doi.org/10.1080/15421406.2021.2013590)

To link to this article: <https://doi.org/10.1080/15421406.2021.2013590>



Published online: 09 Dec 2021.



Submit your article to this journal [↗](#)




View related articles [↗](#)



View Crossmark data [↗](#)



Interaction of hectorite clay with a phospholipid monolayer at air-saline interface in presence of a fluorescent dye

Tanmoy Singha, Ujjal Saren, Pradip Maiti, Utsav Chakraborty, Alapan Pal, and Pabitra Kumar Paul 

Department of Physics, Jadavpur University, Kolkata, India

ABSTRACT



The effect of hectorite clay on the monolayer of 1, 2-dipalmitoyl-sn-glycero-3-phosphocholine (DPPC) at air-saline interface in presence of fluorescent dye acridine orange (AO) is studied. Surface pressure–area isotherm and compressibility studies reveal the phase behavior and rheological properties of DPPC monolayer. Formation of DPPC/clay complex and their aggregation during monolayer compression partially remove DPPC molecules from the interface. UV-vis absorption and fluorescence emission techniques confirm the aggregation of AO in DPPC/clay/AO hybrid Langmuir-Blodgett film. As phospholipids act as lung surfactants, this model study has implication of realizing the detrimental effects of clay on phospholipids during alveolar surface compression while breathing.

KEYWORDS

acridine orange; bio-membrane; DPPC; hectorite; isotherm; Langmuir-Blodgett

1. Introduction

Amphiphilic molecules show interesting surface-active properties and form insoluble monolayer when they are spread at the air water interface. This is known as Langmuir monolayer. Langmuir monolayer has been widely investigated by the analysis of surface pressure versus area per molecule (π -A) isotherm which gives a well-defined, two dimensional media where molecular orientation, packing density, surface tension and phase behavior can be controlled by changing various parameters. Langmuir monolayer is very useful to precisely understand the molecular level interactions especially for various bio-molecular interface such as membranes [1–3]. Nowadays there is big concern about some harmful effects of inorganic layered nanomaterials such as clay minerals on biologicals membranes [4]. Phospholipids are well known as the primary component for bio-membrane and therefore the study of interactions of nanoclay with phospholipid membrane is of major importance. Phospholipid monolayer are used as a fundamental ex-vivo model of a cell membrane but they are also used to explore the interfacial properties of lung (or pulmonary) surfactant (LS) [5]. Respiratory symptoms and undesired health effects are caused by inhalation of dust particles formed from the mineral materials present in the environment. Another complex problem in our health is occurred due to aerosol deposition in our respiratory system [6,7]. As the Langmuir monolayer

CONTACT Pabitra Kumar Paul  pabitra_tu@yahoo.co.in; pabitrak.pal@jadavpuruniversity.in  Department of Physics, Jadavpur University, Jadavpur, Kolkata, 700032, India

© 2021 Taylor & Francis Group, LLC

technique can mimic the bio-membrane, so the interaction of such nano clay may reveal the change of surface behavior of Langmuir monolayer of membrane molecules. This is because the nanometer level size with a large surface area-to-volume ratio of clay may influence the phase behavior and the assembly structure of such Langmuir monolayer at air-water interface. Various type of clays and their possible interactions in biomolecular environment may be used as model system of respiratory physiology [8], bio-membranes [9,10] etc. Therefore, it attracts immense interest to study the effects of clay mineral on the biological system both for fundamental and biomedical interest [11–14].

Here in the present work, we have studied the effects of nano clay particles on the Langmuir monolayer of model lung surfactant phospholipid 1, 2-dipalmitoyl-sn-glycero-3-phosphocholine (abbreviated as DPPC) at the air-saline water interface. DPPC is a zwitterionic phospholipid capable of forming stable Langmuir monolayer at air-water interface. Langmuir monolayer resembles an ideal model for the studies of phospholipids, proteins, pulmonary surfactants, organic, inorganic, and other amphiphilic molecules [7, 15–19] at air-water interface. DPPC is one of the common natural phospholipid and a dominant lipid in mammalian lung surfactant (LS) [20] as well as the common component in a variety of cell membranes. The insoluble DPPC monolayer is a great model system to mimic some of the properties of lung surfactant, such as the surface tension lowering ability during exhalation and the re-spreading ability during inhalation [21]. The properties and phase behavior of Langmuir monolayer of DPPC have been extensively investigated by different type of techniques [22]. The phase transitions of lipid monolayer are very important in respect to their different physiological functions [23,24].

On the other hand, clay, such as smectite (i.e. 2:1 phyllosilicates) are inorganic materials with layered structure. They are functional materials in the scientific field due to interesting properties such as ordered structure, high ion exchange capacity [25], and high surface area to volume ratio. They can efficiently adsorb organic materials on their surfaces and have shown a great promise for the construction of hybrid organic/inorganic nanomaterials. In modern era, organo-clay hybrid film is attracted great attention because of their possible applications in different fields such as electrode modifiers [26–29], sensors [30,31], drug delivery [32–35], etc. Among the various clay materials, hectorite clay is interesting as they have definite layered platelets type structure and negative surface charge and is easily exfoliated in water due to interlayer swelling. In many industrial area as well as our surrounding environment may contain this type of clay as aerosol which can adversely affect our physiological system [36].

In the present study, we have also used cationic dye acridine orange (AO) which is incorporated in DPPC/clay complex Langmuir monolayer formed at air-saline interface. Interaction and association of DPPC and clay in the saline subphase influence the aggregation of AO molecules. Spectroscopic investigations also reveal the aggregation of AO molecules organized in DPPC/clay/AO hybrid LB film [37]. AO has been chosen due to its key role in understanding a wide variety of biochemical processes. Various scientists have focused on the studies of the aggregation behavior of AO in solution and its interaction with biological systems [38]. This planar heterocyclic aromatic compound is used as fluorescent dye in biochemistry, toxicology, molecular biology and supramolecular chemistry [39]. In solution at higher concentration, AO forms aggregates leading to the formation of H-dimer [40]. When AO is adsorbed onto solid substrate

then dimeric sites increased [37]. UV-vis absorption and steady state fluorescence spectroscopic studies have been explored in this work to understand the behavior of AO molecule in hybrid LB film. AFM analysis gives the visual evidence for the morphology and distribution of nanoparticles in the hybrid LB film.

2. Experimental

2.1. Materials

1, 2-dipalmitoyl-sn-glycero-3-phosphocholine (abbreviated as DPPC, MW 734.03, purity >99%) and the cationic dye Acridine Orange (abbreviated as AO) (MW 301.8, purity >99%) were purchased from Sigma-Aldrich Chemical Company, USA and are used in the present work without further purification. However, their purity has been checked spectroscopically namely UV-vis absorption and Fluorescence emission techniques prior to their use in the experiment. Sterile sodium chloride solution (0.9% saline) was prepared using ultra-pure Milli-Q grade water (resistivity of 18.2 M Ω -cm) and autoclaved overnight before use as the subphase for LB experiment and solvent. Clay mineral hectorite was procured from the repository of Clay Mineral Society and was kept in a vacuum desiccator before use. Spectroscopic grade Chloroform was purchased from SRL Chemical Company, India and their purity was also checked by fluorescence emission spectroscopic method before use. The molecular structure of AO and the crystal structure of hectorite are shown in Fig. 1a and b respectively. The molecular structure of DPPC is shown in the inset of Fig. 2.

2.2. Preparation of Langmuir-Blodgett film

Surface pressure versus area per molecule (π -A) isotherms of DPPC in presence of clay and AO at air-saline interface were recorded by Langmuir-Blodgett film deposition

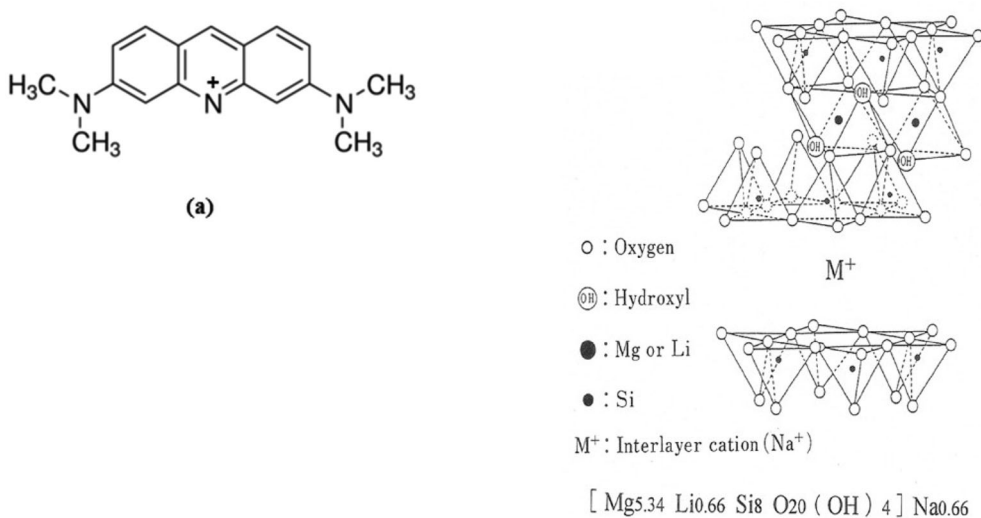


Figure 1. (a) Molecular structure of AO and (b) crystal structure of hectorite clay.

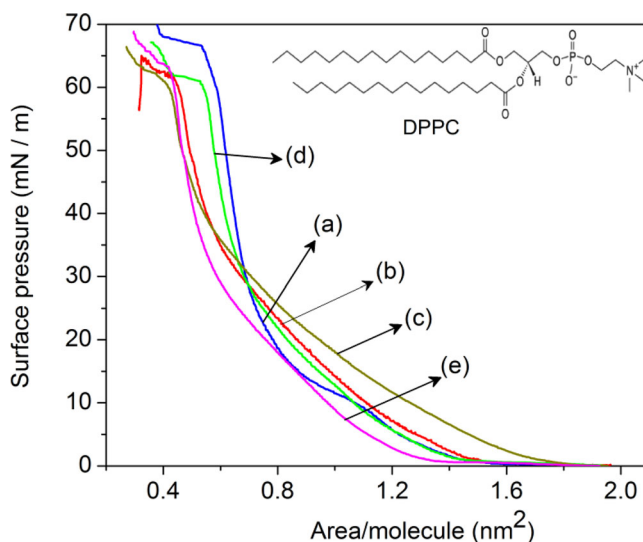


Figure 2. Surface pressure vs. area per molecule (π -A) isotherms of (a) pure DPPC monolayer at air-saline interface in Langmuir trough and DPPC monolayer at air-saline interface of Langmuir trough in presence of various concentration of hectorite clay i.e. (b) 2 ppm (c) 4 ppm (d) 6 ppm and (e) 8 ppm.

instrument (Model LBXD-NT, Make: Apex Instrument Co. Pvt. Ltd., India) using Wilhelmy type film balance technique in a polytetrafluoroethylene (PTFE)-coated Langmuir trough (530 mm \times 165 mm). The Langmuir trough was filled by the saline water subphase for all isotherm studies. The compression and expansion of the subphase surface in the Langmuir trough were symmetrically achieved by means of two movable rectangular shaped Teflon made barriers. The experimental arrangement can essentially mimic the interfacial properties of important model lung surfactant namely DPPC at air-saline interface that is one can realize their dynamical phase behavior in the biological environment. The trough and the barriers of the LB instrument were rigorously and carefully cleaned by triple distilled deionized Milli-Q water (Resistivity 18.2 M Ω -cm) followed by Chloroform prior to start the experiments. Temperature of the subphase in the LB trough remained constant (25 $^{\circ}$ C) throughout the experiment.

In order to obtain surface pressure versus area per molecule (π -A) isotherms at the air-saline water interface in the LB trough, 70 μ l of the dilute chloroform solution of DPPC was spread by a microliter syringe (Hamilton, USA) drop-wise on to the air-saline interface. In addition, hectorite clay was dispersed throughout the saline water subphase containing aqueous solution of AO (100 μ l of concentration of 2 mM) in LB trough. It is expected that the clay nanoparticulate should not aggregate in 0.9% saline subphase because of their typical zeta potential which is known to have negative values in low to medium ionic strength solution [41]. Then after allowing 15 min to evaporate the solvent from the interface, two barriers were compressed slowly i.e. at a rate of 5 mm/min with the help of software controlled computer interface to record the surface pressure-area per molecule (π -A) isotherm. The amount of DPPC spread onto the subphase was low in the experiments so that the isotherm can start from the random gaseous molecular phase of DPPC molecules at air-saline water interface in the selected

trough area. Hectorite clay of varying concentrations (2 ppm, 4 ppm, 6 ppm and 8 ppm etc.) were also dispersed in saline water (used as the LB subphase) containing AO dye molecules. Quartz substrates were thoroughly and carefully cleaned by piranha solution (3:1 mixture of conc. H_2SO_4 and H_2O_2) [42] in an oxidative bath for 30 min and then rinsed with deionized water several times. The substrates were then dried under N_2 air-flow for 10 min and then preserved in the vacuum desiccator until their use in film fabrication. This cleaning procedure is very important in order to remove any organic impurities present in the quartz surface thereby enhancing the hydrophilicity of the substrates by rendering $-\text{OH}$ ions to their surfaces. Langmuir-Blodgett film from pure DPPC and DPPC/clay/AO hybrid molecular assemblies were deposited onto these fluorescence grade quartz substrates by dipping and lifting vertically through the floating Langmuir monolayer at air-saline interface with a speed of 3 mm/min and at a fixed desired surface pressure while keeping the barriers fixed. Mono and multilayered LB films were fabricated onto quartz substrates by repeating the dipping and lifting cycle through the subphase.

2.3. Characterizations

After depositing the mono and multilayered LB films, they were characterized by various analytical techniques. To understand the detailed photophysical behavior of the molecular assemblies organized in LB films, UV-vis absorption spectrophotometer (Model: UV-1800, Make: Shimadzu, Japan) and steady state fluorescence emission spectrophotometer (Model: Fluoromax 4, Horiba Scientific Incorporated, USA) have been used in ambient conditions. ATR-FTIR spectroscopy (Model: Spectrum Two, make: Perkin Elmer Inc. USA) was employed to confirm the interaction between DPPC, hectorite clay and AO dye toward the formation of hybrid Langmuir-Blodgett film on to the solid substrate. The surface morphology of the LB film was studied by Atomic Force Microscopy (Model: Inova, make: Bruker AXS Pte Ltd.) in tapping mode using a silicon cantilever.

3. Results and discussions

3.1. Surface pressure vs. Area per molecule (π -A) Isotherm study

Fig. 2 shows the surface pressure vs. area per molecule (π -A) compression isotherms of pure DPPC monolayer on saline water subphase along with that in presence of hectorite clay of different concentrations in the same saline sub phase on the LB trough. Surface pressure-area isotherm of pure DPPC molecules at air-saline interface shows a slight plateau region between $0.97 - 1.08 \text{ nm}^2$ with an initial liftoff area of 1.47 nm^2 . However, the isotherms are shifted to higher areas at low surface pressures in the air-saline interface containing hectorite clay. This indicates monolayer expansion. The effective attractive interaction between zwitterionic DPPC and clay can approximate the formation of DPPC/clay complex species which requires larger area to organize at air-saline interface leading to the expansion of the monolayer compared to that of pure DPPC. This expansion of the monolayer in the subphase is manifested as the observed increase of initial lift off area of the π -A isotherm of DPPC in presence of hectorite clay. From the figure

it is observed that pure DPPC isotherm has different monolayer phases viz. gaseous (G), Liquid-Expanded (L-E), liquid condensed (L-C) and solid phases (S). The nature of the isotherm is consistent with the data reported elsewhere [43]. The gaseous phase lies in the range of molecular area $\sim 1.6\text{-}1.9\text{ nm}^2$ where the arrangement of phospholipid molecules at air-saline interface are in random direction and the surface pressure did not rise in appreciable amount and the initial liftoff area shows 1.63 nm^2 . This phase corresponds to a condition of less intermolecular cohesive interaction between DPPC molecules. Interestingly above the area/molecule of 1.46 nm^2 the surface pressure begins to rise gradually and the shape of the curve is almost homogeneous in the region of area/molecule of $1.63\text{ }\sim\text{ }1.04\text{ nm}^2$ and this region may be considered as the L-E region where the surface pressure becomes $\sim 10\text{ }\sim\text{ }12\text{ mN/m}$. On further compression of the monolayer there is a slight upward change of the slope of the curve and also surface pressure increases. This phase of DPPC monolayer at air-liquid interface can be regarded as the liquid condensed (LC) phase. But the LE and LC phase can coexist when the molecular area lies between $\sim 1.0\text{ }\text{-}\text{ }0.77\text{ nm}^2$ with the surface pressure ranging between $2\text{-}20\text{ mN/m}$. This indicates some appreciable extent of cohesive intermolecular interactions in the phospholipid monolayer film formed at air-saline interface.

On the other hand, π -A isotherms of DPPC in presence of hectorite clay in the saline subphase at various concentrations show the similar shape but increased liftoff area with increase in clay concentrations up to 4 ppm in the subphase. Moreover, in presence of clay (with concentrations of 2 ppm, 4 ppm and 6 ppm) the isotherms are almost shifted to the larger surface area/molecule when compared to that of pure DPPC monolayer in absence of clay in the subphase. This increase in area/molecule at the interface reveals the possible interaction of clay particulates with the DPPC monolayer at the interface. In fact, hectorite clay is negatively charged in the aqueous saline subphase and so they can electrostatically bound to the zwitterionic DPPC molecules to form complex molecular assemblies at the interface resulting the isotherms to shift toward larger area side. Also interestingly the pleatue like region (which indicates the co-existence of LE-LC phase) in the surface pressure vs area/molecule isotherm of DPPC is totally disappeared in presence of clay. Therefore, the presence of clay definitely corresponds to the change in phase transition upon barrier compression due to more closure association of molecules at the interface when compared to that of pure DPPC. However, on further increase in clay concentration i.e. at 8 ppm the isotherm is again shifted back to the lower area/molecule side in the trough when compared to that of pure DPPC monolayer as shown in Fig. 2. This shift of the monolayer in presence of clay with high concentration in saline water may be due to the aggregation of some fractions of nanoparticulates which were attached with the polar part of DPPC as more and more clays are in contact with DPPC via electrostatic attractive interaction in the aqueous phase. But, due to the presence of more number of clay platelets at the interface some fraction of them may become partly hydrophobic and can aggregate in the liquid phase forming larger sized molecular clusters that can eventually sink [44]. Due to this reason some amount of DPPC molecules which were already complexed with clay at the interface may leave the interface causing the decrease in area/molecule and shift of the isotherm to lower area side.

From Fig. 2, it is also observed that pure DPPC monolayer collapses when the surface pressure approaches to 66 mN/m at area per molecule of 0.46 nm^2 . The collapse of the

monolayer film occurs due to the formation of aggregates or clusters of DPPC at such higher surface pressure because of their closure association and attractive cohesive intermolecular interactions in the solid phase of the isotherm. On the other hand, in presence of clay platelets the mixed or complex isotherms do not show any significant change in the collapse pressure. The horizontal portion of the DPPC in the region of area per molecule of $0.42\text{--}0.37\text{ nm}^2$ is most probably due to the fact that some amount of DPPC leaves the interface layer as a result of the formation larger aggregates or molecular clusters at the air-saline interface at very high surface pressure.

The interaction between the clay platelets and the DPPC molecules may also be understood by the incorporation of fluorescent dye probe such as AO used in this work. Because the clay/phospholipid assemblies may eventually influence the organization and association of AO in the hybrid interface. Fig. 3a shows the surface pressure vs. area per molecule isotherms of DPPC monolayer in the saline subphase containing $100\ \mu\text{l}$ aqueous solution of AO and hectorite clay with various concentrations viz. 0 ppm, 2 ppm, 4 ppm and 6 ppm. The concentration of AO solution was 2 mM for each of these isotherm studies. Pure DPPC monolayer has four distinct phases with initial liftoff area of about 1.42 nm^2 in presence of AO dye without clay in the saline subphase. But in the presence of both AO and hectorite clay (concentration of 2 ppm) in the subphase the isotherm shifts to sufficiently lower area with the decrease in the initial liftoff area of 1.13 nm^2 . This decrease in area per molecule in all phases of the monolayer at air-saline interface suggesting that clay-dye complex nanoparticulate could have effectively shortened the distance between DPPC molecules. As a result, the monolayer may be more densely packed covering the lower surface area in the LB trough compared to that in absence of clay at the air-saline interface. The clay platelets are negatively charged in the subphase and AO is positively charged and so initially most of the AO molecules could be adsorbed onto the clay surface via electrostatic interaction. When the DPPC solution was spread onto the subphase the complex clay/dye species interacts with polar moieties of DPPC. However, clay/dye complex molecular species also hydrophilic and as the DPPC is zwitterionic the polar part of which can interact with the AO differently in the subphase leaving their hydrocarbon chain outside (air) the subphase surface. Additionally, AO molecules may also aggregate on the clay surface which can disrupt the balance between the hydrophobic and hydrophilic interaction of DPPC at air-saline interface. Therefore, some fraction of DPPC might have dissolved into the subphase resulting the decrease in surface area and it can also affect the rigidity of the hybrid monolayer at the interface. This is further explained later in terms of 2-D compressional modulus as shown in Fig. 3b. However, the nature of the observed shift of π -A isotherm of DPPC in presence of AO and hectorite clay clearly depends on the clay concentrations in the given subphase. Interestingly, on further increase of concentration of hectorite clay keeping the dye concentration fixed in the subphase, the isotherm now tends to shift toward higher surface area side in the Langmuir trough. As the amount of dye is fixed in the subphase, more number of clay particulate may come at the interface causing the increase in the average molecular area of DPPC in the interface. Therefore, the increase in surface area of the monolayer at higher clay concentration is possibly due to the presence of more number of clay/dye complexed nanoparticulates in the monolayer. Also in presence of clay and dye the distance

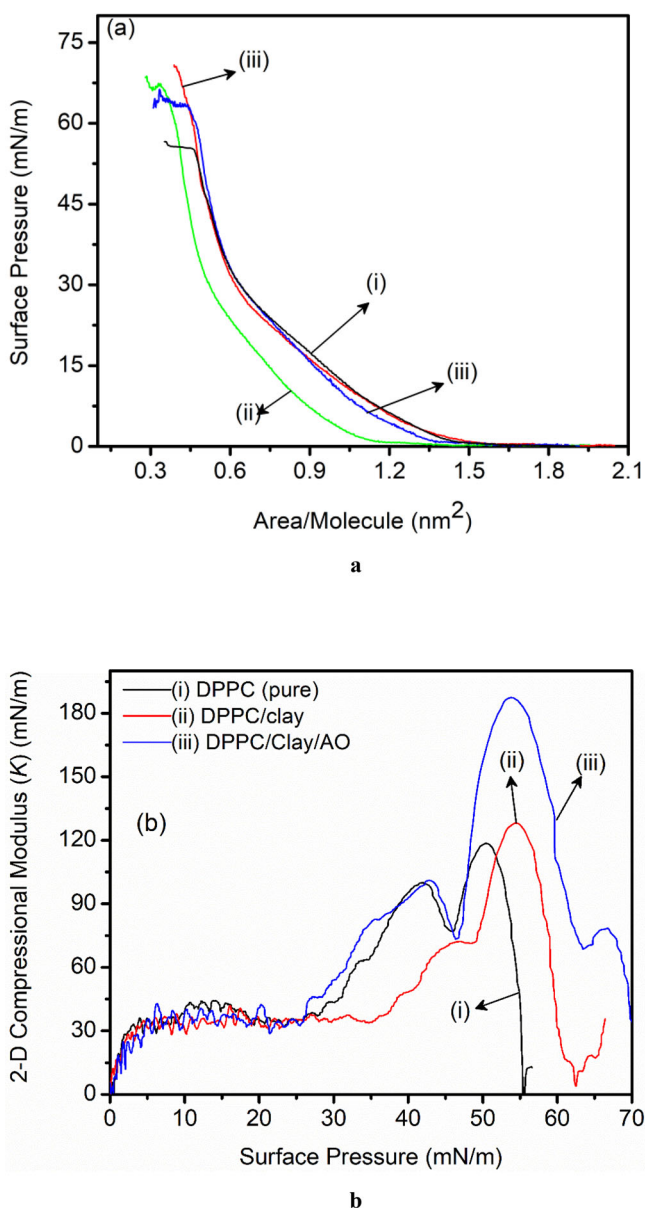


Figure 3. a: Surface pressure vs. area per molecule (π -A) isotherms of DPPC on the surface of 0.9% saline subphase containing different concentrations of hectorite clay viz. (i) 0 ppm (ii) 2 ppm (iii) 4 ppm and (iv) 6 ppm. The subphase also contains 100 μ l of AO aqueous solution in each case before spreading the DPPC solution in the LB trough. b: Plot of 2-dimensional surface compressional modulus (K) as a function of surface pressure for Langmuir isotherm of pure DPPC monolayer, DPPC/clay mixed monolayer and DPPC/clay/AO hybrid monolayer.

between DPPC headgroup might have increased. However, the optimum concentration of the dye molecules adsorbed onto DPPC monolayer is stabilized by the chemical potential of the dye with that in the mixed or hybrid monolayer at the saline subphase so that a dynamic equilibrium is established [45].

To understand the rheological properties of the monolayer phases of the model lung surfactant DPPC at the air-saline interface and the effect of clay mineral in presence of a cationic fluorescent probe (AO), 2-D surface compressional modulus (K) have been explained in this work. This is defined on the basis of π -A isotherm characteristics of the monolayer and is given by the equation [46]:

$$K = -A \left(\frac{d\pi}{dA} \right)_T \quad (1)$$

where, A is the area per molecule at any particular surface pressure of the monolayer at the air-liquid interface at constant temperature. The reciprocal of the surface compressional modulus (K) is known as the compressibility (C) [46,47] of the monolayer and is sometimes used to characterize the mechanical properties of the monolayer at air-liquid interface i.e.

$$C = \frac{1}{K} = -\frac{1}{A} \left(\frac{dA}{d\pi} \right)_T \quad (2)$$

As mentioned earlier about the monolayer phases i.e. Gaseous, L-E, L-C and Solid phases manifested in the π -A isotherm, the surface compressional modulus (K) can be calculated for the monolayer elasticity as well as to probe the molecular level interactions toward the formation of superficial molecular architectures at the air-saline interface.

Fig. 3b shows the 2-dimensional compressional modulus (K) as a function of surface pressure of pure DPPC monolayer at air-saline subphase, the saline subphase containing hectorite clay dispersion and clay/dye mixed saline subphase. From this figure it is observed that initially the 2-D surface compressional modulus increases as the compression of the monolayer by the movable barriers at air-saline interface and when reached approximately at 38 mN/m it became constant up to the surface pressure of about 25 mN/m. The initial lower values of the K resemble to the fact that the monolayer is in gaseous phase and subsequently in the liquid phase and so both the phases are highly compressible. This also corresponds to less intermolecular interactions at the interface. Beyond the surface pressure of 26 mN/m, both DPPC and DPPC/Clay/AO interfacial monolayer again start to increase but the rate of increase of K in case of DPPC/Clay/AO hybrid molecular assemblies is faster than that of pure DPPC at air-saline interface. This higher value of K of the hybrid molecular assemblies corresponds to the formation of more rigid interfacial layer compared to pure DPPC monolayer in the absence of AO and clay in the subphase. It should also be emphasized here that the sudden change in values of K after surface pressure of 26 mN/m clearly reveals the phase transition from L-C state to the onset of solid or aggregated phase. At the surface pressure of around 42 mN/m for both the monolayer, there is abrupt fall of K from 100 mN/m to 75 mN/m. This sudden decrease of K at high surface pressure reveals the removal of surface active components from the interface to the subphase due to the formation of aggregated structure of both the dye molecules and DPPC in the hybrid monolayer. On further compression after reaching the surface pressure of 45 mN/m the monolayer became densely packed which corresponds to the increase in K value and finally a fall from 50 mN/m and 55 mN/m for DPPC and DPPC/Clay/AO hybrid molecular assemblies

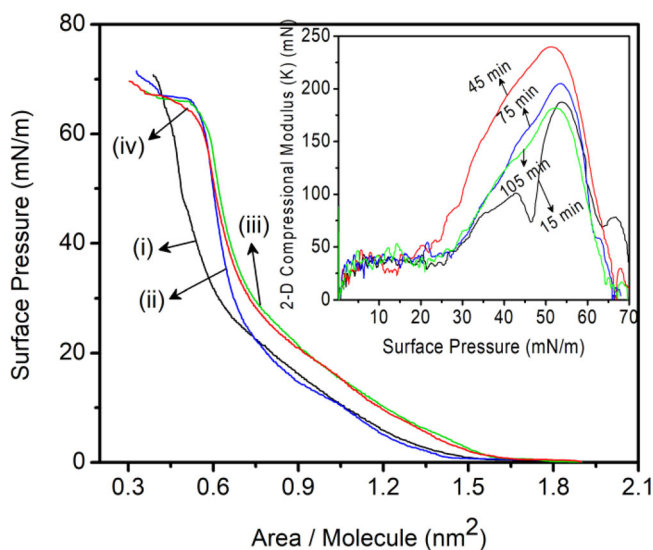


Figure 4. Plot of Surface pressure vs. area per molecule (π -A) isotherms of DPPC/Clay/AO hybrid Langmuir monolayer on the surface of 0.9% saline subphase recorded at different incubation time viz. (i) 15 min, (ii) 45 min, (iii) 75 min and (iv) 105 min after spreading DPPC solution onto the subphase. Concentration of hectorite clay and AO dye in the subphase were 4 ppm and 2 mM respectively. Volume of AO aqueous solution in the subphase was containing different hectorite clay was 70 μ l AO. Inset shows the 2-Dimensional Compressional Modulus (K) of the hybrid Langmuir monolayer at air-saline interface as a function of surface pressure recorded at different time elapsed of spreading DPPC in the subphase.

respectively. The sharp fall of K indicates the collapse of the monolayer due to the formation of multilayers or clusters throughout the subphase surface.

On the other hand, DPPC/clay complex monolayer is somewhat more compressible in the initial phase (G, L-E, L-C). But in the later phase (after surface pressure of 38 mN/m) the monolayer is more rigid and collapsed at higher surface pressure compared to those of pure DPPC.

The effect of subphase incubation time after spreading the DPPC molecules onto Clay/dye mixed saline subphase is also studied in the present work. Fig. 4 shows the π -A isotherms of DPPC monolayer run after different time namely 15 min, 45 min, 75 min and 105 min after spreading the DPPC solution onto Clay/dye mixed saline subphase. From the figure it is observed that the isotherms run after 15 min and 45 min of spreading the sample solution are almost similar except that the area per molecule at solid phase (after surface pressure of 22 mN/m) of the isotherm recorded after 45 min is higher compared to that after 15 min. This observation clearly reveals that more number of clay/dye complex come at the interface with increase in time and become highly condensed after barrier compression because the isotherm becomes much steeper at the solid phase. That is with increase in time of adsorption of the dye/clay complex molecular systems the cohesive interaction between DPPC polar head group increases thereby causing more compactness of the hybrid molecular assemblies at the interface. However, on further increase in subphase incubation time i.e. 75 min and 105 min before running the isotherm but after spreading the DPPC solution in the clay/AO dispersed saline subphase, the isotherms span in the higher surface area in the Langmuir

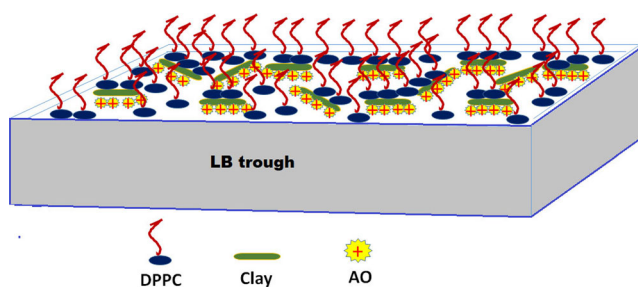


Figure 5. Schematic presentation of the formation of the DPPC/Clay/AO complex hybrid Langmuir monolayer at air-saline interface.

trough. This observation basically implies the more closure association of the hybrid molecular species at the interface thereby increasing the molecular interaction at the early phase of the monolayer. However, the nature of interaction may be the same as the similar shape of the isotherm when recorded at smaller time after subphase incubation.

To have a better understanding of the effect of subphase incubation time before the barrier compression on the possible involved interaction and various phases during the formation of the hybrid molecular assemblies at air-saline interface, the 2-D surface compressional modulus versus surface pressure has been plotted as shown in the inset of Fig. 4. From this figure, it is clear that up to the surface pressure of 20 mN/m the phase behavior and the corresponding elastic properties are very similar for the monolayer with the various subphase incubation time namely, 15 min, 45 min, 75 min and 105 min. The formation of DPPC/Clay/AO hybrid Langmuir monolayer at air-saline interface is schematically shown in Fig. 5.

3.2. *Uv-Vis absorption spectroscopic study*

In the present work, we have also deposited the LB film of DPPC/Clay/AO bio-organo-clay hybrid molecular assemblies on to the quartz substrate by vertical deposition (Y-type) method from the air-saline interface. To understand the molecular organization as well as molecular mechanism in the ground electronic states of the adsorbed dye molecules in hybrid LB films, UV-vis absorption spectroscopic study was performed. Fig. 6a shows the UV-Vis absorption spectra of 10-layered DPPC/Clay/AO hybrid LB films deposited onto quartz substrate at a surface pressure of 15 mN/m along with pure bulk microcrystal and pure aqueous solution of AO for comparison. From the figure, it is observed that pure AO solution has strong monomeric absorption band with peak centered at around 490 nm along with a weak shoulder at 470 nm. These results are in well agreement with the studies reported elsewhere [48]. The weak absorption band at 470 nm of AO solution is mainly due to the presence of some dimeric units of dye molecules present in the solution phase [49]. This type of dimers of AO are generally referred to as the H-dimers or aggregates [50]. On the other hand, absorption spectrum of DPPC/Clay/AO hybrid LB film shows the same monomeric band at 490 nm but having relatively reduced intensity along with an additional absorption band observed at 400 nm which is possibly due to the sandwiched type (H-type) of aggregates or stacking

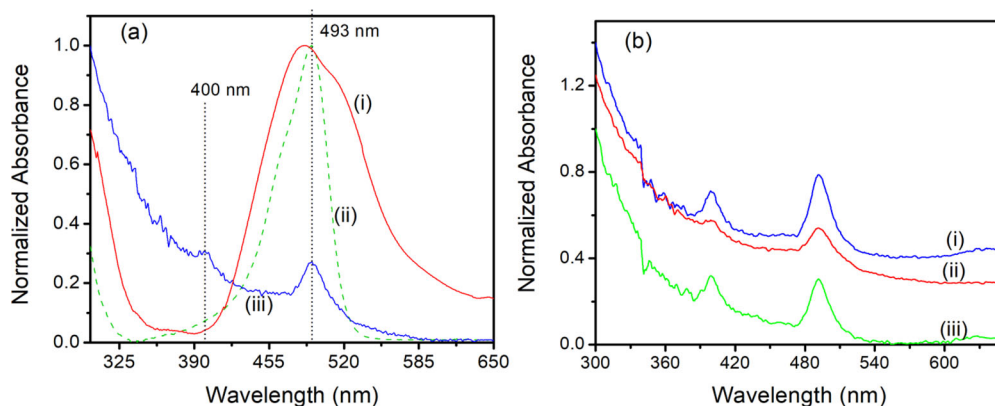


Figure 6. (a) UV-vis absorption spectra of (i) AO bulk microcrystal film deposited onto quartz substrate, (ii) AO aqueous solution and (iii) 10 layered DPPC/Clay/AO LB film deposited onto quartz substrate at surface pressure of 15 mN/m. (b) UV-vis absorption spectra of 10 layered DPPC/Clay/AO LB film deposited onto quartz substrate at surface pressure viz, (i) 15 mN/m, (ii) 10 mN/m and (iii) 25 mN/m respectively.

of dye molecules in the hybrid LB film [51]. The blue shifting of the dimeric absorption band of AO in case of LB film when compared to that of pure AO solution may be attributed to the closer association of the dye molecules due to the interaction of clay platelets in the zwitterionic DPPC head group in LB film. That is in LB film the relative distance between dye molecules are reduced and facilitates more enhanced interactions between the electric transition dipole moments of dye molecules when interacts with light. It is already known that clay platelets have very high tendency to facilitate aggregation of various cationic dye molecules due to the presence of negative surface charge in the clay platelets [52]. The absorption spectrum of AO bulk microcrystal spread onto quartz substrate shows the monomeric band at around 484 nm along with a new vibronic shoulder at 516 nm. The slight blue shifting of monomeric absorption band for AO microcrystal is most possibly due to closer association of dye molecules in the bulk solid phase. The vibronic shoulder is mainly attributed to the associated vibronic transition along with electronic transition as a result of overlapping of several vibrational energy levels corresponding to each electronic energy states and consequently the spectrum become more broadened than that of LB film or solution.

Fig. 6b shows the normalized UV-Vis absorption spectra of 10-layered DPPC/Clay/AO LB films deposited onto quartz substrate at various surface pressure namely 10 mN/m, 15 mN/m and 25 mN/m. All the absorption spectra show the same monomeric band at 490 nm along with the higher energy band at 400 nm, except a little change in their intensity distribution. As mentioned earlier, this band is probably due to the parallel stacking of AO monomer units in between the DPPC chain and their aggregations were influenced by Clay platelets present in the hybrid LB film.

3.3. Steady state fluorescence spectroscopic study

From the isotherm study, it is already observed that the nanoplatelets clay has the substantial effects on the surface properties of DPPC at air-saline interface. Additionally,

the fluorescent dye AO also successfully adsorb in the complex Langmuir monolayer thereby forming the hybrid Langmuir monolayer which was successfully transferred onto solid substrate to prepare the hybrid LB film. AO molecules were attached to the clay platelets via electrostatic interaction and the aggregation of dye molecules occurred in LB films and is reflected on their optical absorption spectra, which are confirmed by UV-Vis absorption spectroscopic technique. However, to have further knowledge of the molecular mechanism involved in their electronic states, steady state fluorescence emission studies were also performed. Fig. 7a shows the normalized steady state fluorescence spectra of 10-layered DPPC/Clay/AO LB film deposited onto quartz substrate at a surface pressure of 15 mN/m along with that of pure AO solution and microcrystal for comparison. The excitation wavelength for all these samples were considered at 480 nm with unaltered slit-width in all the cases. Pure AO aqueous (curve i) solution shows a strong fluorescence emission band centered at around 525 nm when excited at 480 nm. But in the case of LB film (curve ii), this peak has been shifted to 515 nm. Interestingly, the AO microcrystal emission spectrum also exhibit emission band at 505 nm, which definitely corresponds to the formation molecular aggregates of AO because of much closure association of the molecules in the solid state. So, the shift of the emission peak in case of LB film and bulk microcrystal compared to that of pure AO solution might be due to the aggregation of dye molecules. Fig. 7b shows the normalized Steady state fluorescence spectra of 10-layered DPPC/Clay/AO hybrid LB films deposited on to quartz substrate at surface pressure of 15 mN/m through the saline subphase containing hectorite clay of various concentrations viz. 2 ppm, 4 ppm, 6 ppm, 8 ppm respectively. It is interesting to note that the emission spectra of 10 layered LB films deposited from various clay concentrations show almost similar band pattern but only with increase in their intensity distribution. This observation indicates that nano clay particulates were successfully incorporated between AO and DPPC molecules at the air-saline interface, which was then transferred onto solid substrates for fabrication of LB film. From our study it is also evident that microcrystalline domains are formed in the LB film with increasing clay concentration.

On the other hand, Fig. 7(c) Shows normalized steady state fluorescence spectra of DPPC/clay/AO LB films deposited on to quartz substrate at various surface pressure viz. 10 mN/m, 15 mN/m, 25 mN/m and 35 mN/m respectively. Concentration of Clay in the subphase was 4 ppm at room temperature for fabrication of all these LB films. Pressure effect study of LB film is important because, the morphology and crystal parameter of the film can be controlled by varying the surface pressure of lifting the LB film through the subphase. From these spectra we observe the strong fluorescence emission band centered at 515 nm (which is originated due to 0-0 electronic transition) for the LB films lifted at lower surface pressure namely 10 mN/m and 15 mN/m. However, in case of LB films deposited at higher surface pressure such as 25 mN/m and 35 mN/m the 515 nm band is totally absent rather only emission band centered at 503 nm is present. This may be due to the aggregation of AO molecules in LB films. Because at high surface pressure while depositing the LB films aggregated domains can further stack one above another forming cluster or multilayers of larger dimensions.

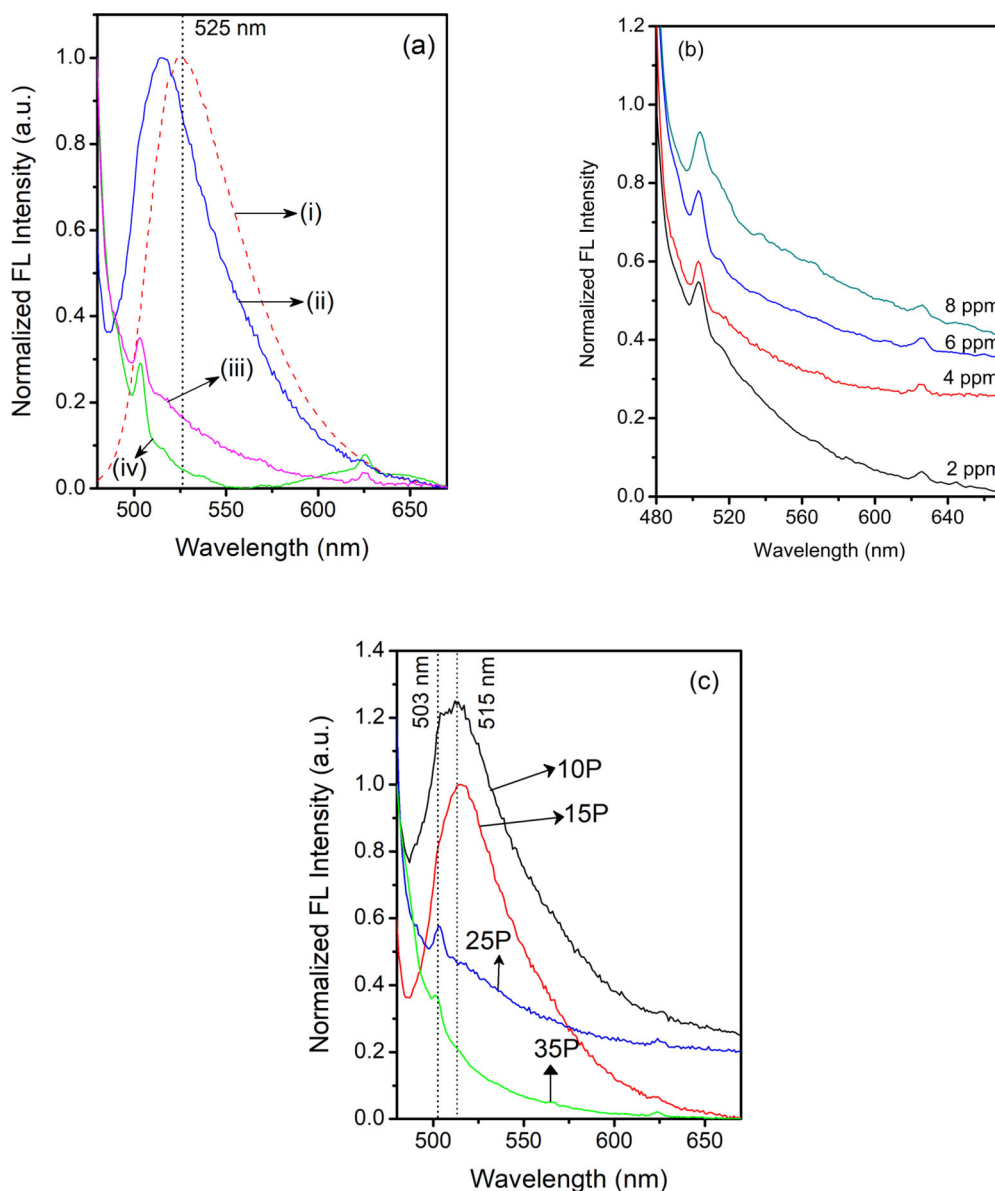


Figure 7. (a) Steady state fluorescence spectra of (i) AO solution, (ii) DPPC/AO mixed LB film deposited onto quartz substrate at surface pressure of 15 mN/m, (iii) DPPC/Hect/AO mixed LB film deposited onto quartz substrate (clay concentration was 4 ppm) at surface pressure of 15 mN/m and (iv) pure AO bulk microcrystal film deposited onto quartz substrate. (b) Steady state fluorescence spectra of 10 layered DPPC/Hect/AO LB films deposited on to quartz substrate at surface pressure of 15 mN/m from Langmuir subphase containing Hectorite clay of various concentration viz 2 ppm, 4 ppm, 6 ppm, 8 ppm respectively. (c) Steady state fluorescence spectra of DPPC/clay/AO LB films deposited on to quartz substrate at various surface pressure viz. 10 mN/m, 15 mN/m, 25 mN/m and 35 mN/m. Concentration of clay in the subphase was 4 ppm at room temperature.

3.4. Atr-FTIR spectroscopic study

The Fourier transform infrared (FTIR) is an excellent spectroscopic method that can identify the molecular level interaction by knowing various molecular bond-vibration after interacting with infrared light. In our experiments measurements were done by the FTIR spectrophotometer in the mid-infrared region (MIR) i.e. in the range of 400-4000 cm^{-1} . Fig. 8 (i) shows ATR-FTIR spectra of pure hectorite clay where the broad band at 3416 cm^{-1} and 3678 cm^{-1} are assigned to the H-O-H bending and stretching vibrations respectively, which indicate that some amounts of adsorbed water molecules might have present in the hydration shell of the Na⁺ cation in the interlayer spaces of the hectorite clay [53]. 975 cm^{-1} band is related to the bending as well as symmetric and asymmetric stretching modes of Si-O-Si respectively. The curve (ii) shows ATR-FTIR spectrum of pure AO which gives distinct vibrational band at around 1592 cm^{-1} which is due to the characteristics of skeletal vibration of the phenyl ring of AO and the band around 3460 cm^{-1} is attributed to the N-H stretching vibration [54]. However, for LB film these bands are not observed may be due to the aggregated structure of the DPPC molecules in the restricted geometry of the solid state. Curve (iii) shows the ATR-FTIR spectrum of DPPC/clay hybrid LB film (10 layer) deposited at a surface pressure of 15 mN/m. There are no such prominent vibrational peaks observed except a peak observed at around 1744 cm^{-1} due to carbonyl group (C=O) along with a very less intense peak observed at 1364 cm^{-1} . Also there is no symmetric PO_2^-

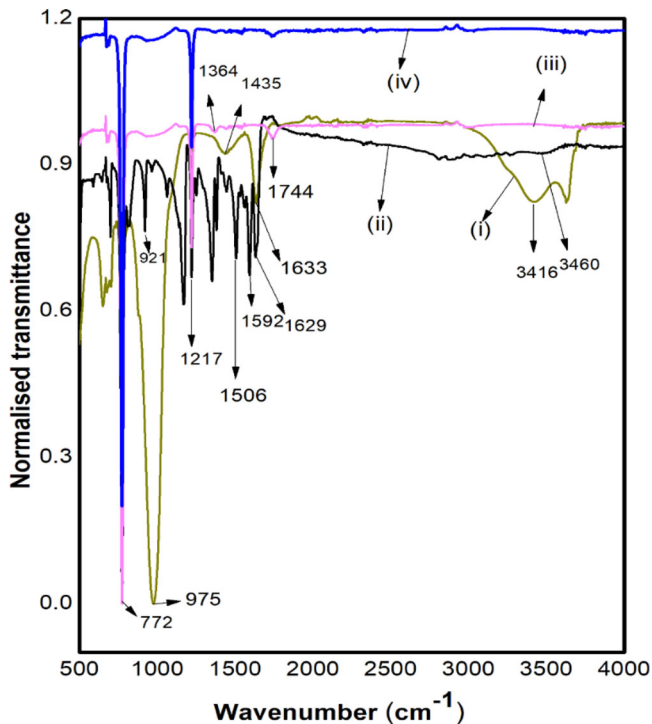


Figure 8. ATR-FTIR spectra of (i) pure hectorite, (ii) pure AO, and 10 layered LB film of (iii) DPPC/clay, (iv) DPPC/clay/AO deposited onto glass substrate at surface pressure of 15 mN/m and concentration of clay was 4 ppm in Langmuir subphase.

stretching vibration band at 1090 cm^{-1} due to the absorption of DPPC molecules in the clay surface [55,56]. On the other hand, ATR-FTIR spectrum (curve iv) of DPPC/clay/AO hybrid LB film (10 layer) deposited at a surface pressure of 15 mN/m shows only strong transmission peaks at around 772 cm^{-1} and 1217 cm^{-1} indicating the adsorption of AO molecules in the hybrid LB film.

3.5. Atomic force microscopic study

Atomic force microscopy is now an elegant method for understanding the surface morphology including roughness and thickness of nano-dimensional film of various biological and other different materials deposited onto solid substrate. The morphology and surface structure of the DPPC/clay/AO hybrid LB films deposited on smooth Silicon wafer at two different surface pressure were studied by a commercially available Atomic force microscope (AFM) in tapping mode as shown in Fig. 9(a) and (b). At lower surface pressure i.e. 15 mN/m the clay particulates are randomly distributed in the DPPC/Clay/AO hybrid LB film as shown in Fig 9(a), which definitely confirms the attachment of clay particulates with positively charged DPPC molecules in the LB film. The average height of the film was measured as 1.5 nm . However, some interesting results are obtained from the AFM image of DPPC/clay/AO hybrid monolayer LB film lifted at 25 mN/m as shown in Fig 9(b). The AFM image of the hybrid LB films shows dense and compact organization of the DPPC/clay/AO complex structures. Here the clay platelets are almost in contact with each other. As a result, the adsorbed dye molecules might have aggregated structures due to much closure association as consistent with the spectroscopic results. The average height through the measured line is found to be almost 22 nm . The surface coverage is more than 80%. It further indicates the successful incorporation of nano clay platelets into the hybrid LB film.

4. Conclusion

In conclusion, our results show that the presence of anionic clay hectorite highly influence the phase behavior and interfacial properties of the studied phospholipid monolayer and it significantly depends on at air-saline interface. Also the incorporation of fluorescent cationic dye acridine orange (AO) successfully revealed the interaction between dye, clay and the phospholipid monolayer as evidenced from the surface pressure vs area per molecule isotherm and spectroscopic methods. Our study confirms the formation of DPPC/clay/AO hybrid Langmuir monolayer at air-saline interface and successful transfer of hybrid monolayer onto solid substrate. From the study, it is clear that the effective attractive interactions between negatively charged hectorite clay and zwitterionic DPPC forms the DPPC/clay complex species which requires larger area to organize at air-saline interface. Our observations also reveal that DPPC molecules are adsorbed on the surface of nano clay hectorite to form DPPC/clay complexes, which can further aggregates during monolayer compression. This leads to the partial removal of the phospholipid from the interface and indicates destructive effect of nano clay mineral on the DPPC film formed at air-saline interface. Also the aggregation of AO molecules disrupts the balance between hydrophobic and hydrophilic interaction. Presence of

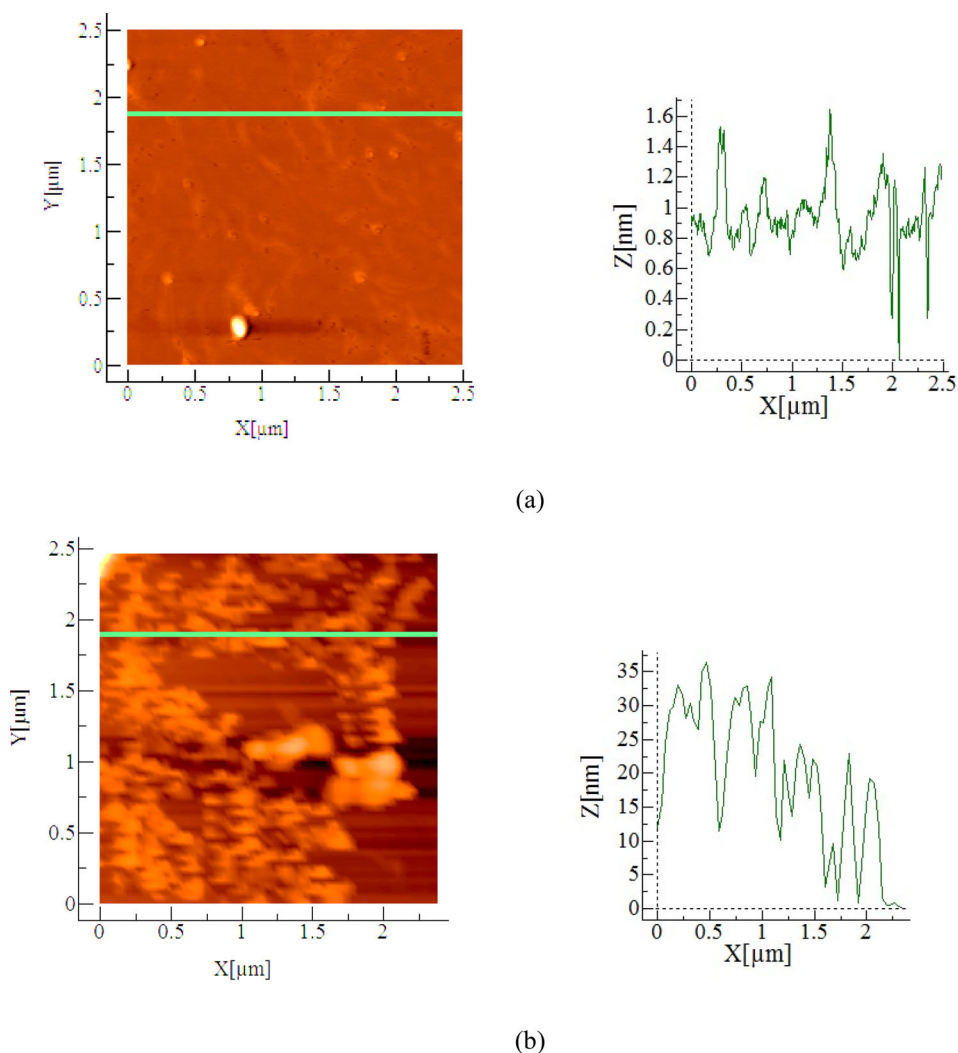


Figure 9. Tapping mode Atomic Force microscopic images (AFM) of one layer hybrid Langmuir-Blodgett film of (a) DPPC/Clay/AO deposited at surface pressure of 15 mN/m and (b) DPPC/Clay/AO hybrid molecular systems deposited onto quartz substrate at surface pressure of 25 mN/m. Concentration of clay in the subphase was 4 ppm. Temperature of the subphase was 25 °C.

clay and AO facilitates more compactness of DPPC monolayers as confirmed by compressibility study. As the phospholipid works as a lung surfactant system in our body it can therefore be argued that presence of such clay or dye eventually interfere with the properties and functions of the phospholipid in our respiratory system in-vivo. Our study reveals that amounts of the phospholipids at the air-saline interface were reduced due to interaction of nanoclay hectorite. This in-vitro study can be a model study which implicate the reduction of surface tension of surfactant molecules in presence of clay particulates during alveolar surface compression associated with exhalation of air while breathing. UV-Vis absorption and steady state fluorescence study further confirms the aggregation of the fluorescent probe AO in the hybrid LB film. FTIR study further

confirmed the interaction of clay and dye with DPPC assembled in LB film. AFM images show clear visual evidence of the surface morphology and distribution of clay in the hybrid LB film.

Acknowledgments

Authors are also thankful to Dr. Partha Roy of the Department of Chemistry, Jadavpur University for providing access of FTIR instrument used in the present work.

Declaration of competing interest

The authors declare that they have no known competing financial interests that could have appeared to influence the work reported by author.

Funding

The author P.K. Paul is grateful to DST for financial support through SERB-DST (Project Ref. No. SB/EMEQ-142/2014) to carry out this research work.

ORCID

Pabitra Kumar Paul  <http://orcid.org/0000-0002-3490-525X>

References

- [1] E. A. Montanha *et al.*, *Biophys. Chem.* **153** (2-3), 154 (2011). doi:10.1016/j.bpc.2010.10.010
- [2] C. Peetla, and V. Labhasetwar, *Mol. Pharmaceutics* **5** (3), 418 (2008). doi:10.1021/mp700140a
- [3] C. Peetla, and V. Labhasetwar, *Langmuir* **25** (4), 2369 (2009). doi:10.1021/la803361y
- [4] D. B. Warheit *et al.*, *Toxicol. Sci.* **77** (1), 117 (2004). doi:10.1093/toxsci/kfg228
- [5] M. Amrein, A. von Nahmen, and M. Sieber, *Eur. Biophys. J.* **26** (5), 349 (1997). doi:10.1007/s002490050089
- [6] M. S. Bakshi *et al.*, *Biophys. J.* **94** (3), 855 (2008). doi:10.1529/biophysj.107.106971
- [7] H. Mohwald, *Annu. Rev. Phys. Chem.* **41** (1), 441 (1990). doi:10.1146/annurev.pc.41.100190.002301
- [8] R. Wustneck *et al.*, *Adv. Colloid Interfaces Sci.* **117** (1-3), 33 (2005). doi:10.1016/j.cis.2005.05.001
- [9] Y. Y. Zuo *et al.*, *Biochim. Biophys. Acta* **1778** (10), 1947 (2008). doi:10.1016/j.bbamem.2008.03.021
- [10] A. D. Bangham, C. J. Morley, and M. C. Phillips, *Biochim. Biophys. Acta.* **573** (3), 552 (1979). doi:10.1016/0005-2760(79)90229-7
- [11] R. K. Harishchandra, M. Saleem, and H.-J. Galla, *J. R Soc. Interface* **7** (suppl_1), S15 (2010). doi:10.1098/rsif.2009.0329.focus
- [12] L. Mazzola, *Nat. Biotechnol.* **21** (10), 1137 (2003). doi:10.1038/nbt1003-1137
- [13] P. H. Hoet, I. Brüske-Hohlfeld, and O. V. Salata, *J. Nanobiotechnol.* **2** (1), 12 (2004). doi:10.1186/1477-3155-2-12
- [14] T. Kanishtha, R. Banerjee, and C. Venkataraman, *Environ. Toxicol. Pharmacol.* **22** (3), 325 (2006). doi:10.1016/j.etap.2006.05.003
- [15] H. Mohwald, *Rep. Prog. Phys.* **56**, 653 (1993).

- [16] H. Nakahara *et al.*, *Langmuir* **22** (3), 1182 (2006). doi:10.1021/la0524925
- [17] H. Nakahara *et al.*, *Langmuir* **26** (23), 18256 (2010). doi:10.1021/la103118d
- [18] M. Mahato *et al.*, *Colloids Surfaces A Physicochem. Eng. Aspects* **414**, 375 (2012). doi:10.1016/j.colsurfa.2012.08.064
- [19] B. Balaswamy *et al.*, *Langmuir* **28** (50), 17313 (2012). doi:10.1021/la303549z
- [20] P. O. Nkadi, T. A. Merritt, and D. M. Pillers, *Mol. Genet. Metab.* **97** (2), 95 (2009). doi:10.1016/j.ymgme.2009.01.015
- [21] J. C. Watkins, *Biochim. Biophys. Acta* **152** (2), 293 (1968). doi:10.1016/0005-2760(68)90037-4
- [22] A. J. Sheridan *et al.*, *Langmuir* **33** (39), 10374 (2017). doi:10.1021/acs.langmuir.7b01077
- [23] B. Maherani *et al.*, *Food Chem.* **134** (2), 632 (2012). doi:10.1016/j.foodchem.2012.02.098
- [24] H. Nakahara *et al.*, *Soft Matter* **7** (24), 11351 (2011). doi:10.1039/c1sm06345f
- [25] D. Varade, and K. Haraguchi, *Langmuir* **29** (6), 1977 (2013). doi:10.1021/la3044945
- [26] Z. Salmi, K. Benzarti, and M. M. Chehimi, *Langmuir* **29** (44), 13323 (2013). doi:10.1021/la402710r
- [27] T. Gan *et al.*, *J. Agric. Food Chem.* **58** (16), 8942 (2010). doi:10.1021/jf101531c
- [28] Y. Chang *et al.*, *Ind. Eng. Chem. Res.* **53** (1), 38 (2014). doi:10.1021/ie402226z
- [29] A. Maghear *et al.*, *Talanta* **125**, 36 (2014). doi:10.1016/j.talanta.2014.02.042
- [30] D. Dey *et al.*, *Sens. Actuators B* **195**, 382 (2014). doi:10.1016/j.snb.2014.01.065
- [31] D. Dey *et al.*, *Sens. Actuators B* **184**, 268 (2013). doi:10.1016/j.snb.2013.04.077
- [32] S. M. Lee, and D. Tiwari, *Appl. Clay Sci.* **84**, 59 (2012).
- [33] C. Guzzi *et al.*, *Appl. Clay Sci.* **36** (1-3), 22 (2007). [Database] doi:10.1016/j.clay.2006.06.015
- [34] M. J. A. Oliveira *et al.*, *Radiat. Phys. Chem.* **94**, 194 (2014). doi:10.1016/j.radphyschem.2013.05.050
- [35] C. Viseras *et al.*, *Appl. Clay Sci.* **48** (3), 291 (2010). doi:10.1016/j.clay.2010.01.007
- [36] M. Datta, *Appl. Clay Sci.* **85**, 80 (2013).
- [37] J. Bhattacharjee, S. A. Hussain, and D. Bhattacharjee, *Spectrochim. Acta Part A* **116**, 148 (2013). doi:10.1016/j.saa.2013.07.018
- [38] C. Xia *et al.*, *Desalination* **265** (1-3), 81 (2011). doi:10.1016/j.desal.2010.07.035
- [39] A. Ulman, *An Introduction to Ultrathin Organic Films: From Langmuir-Blodgett to Self-Assembly* (Academic Press, New York, 1991).
- [40] F. Wang *et al.*, *J. Lumin.* **21** (1), 49 (2006). doi:10.1002/bio.883
- [41] F. Mousseau *et al.*, *Langmuir* **31** (26), 7346 (2015). doi:10.1021/acs.langmuir.5b01639
- [42] K. S. Koh *et al.*, *Micromachines* **3** (2), 427 (2012). doi:10.3390/mi3020427
- [43] Y. Y. Zuo *et al.*, *Langmuir* **32** (33), 8501 (2016). doi:10.1021/acs.langmuir.6b01482
- [44] E. Tombacz *et al.*, *Org. Geochem.* **35** (3), 257 (2004). doi:10.1016/j.orggeochem.2003.11.002
- [45] I. C. Shich, and J. A. Zasadzinski, *PNAS* **112**, 826 (2015).
- [46] D. Vollhardt, and V. B. Fainerman, *Adv. Colloid Interface Sci. Colloid* **127** (2), 83 (2006). doi:10.1016/j.cis.2006.11.006
- [47] B. Dey *et al.*, *Org. Electron.* **55**, 50 (2018).
- [48] A. M. Amado *et al.*, *J. Lumin.* **178**, 288 (2016). doi:10.1016/j.jlumin.2016.06.006
- [49] J. Mondek *et al.*, *Langmuir* **30** (29), 8726 (2014). doi:10.1021/la502011s
- [50] E. Jiménez-Millán *et al.*, *Langmuir* **27** (24), 14888 (2011). doi:10.1021/la2030236
- [51] W. F. Jayen, S. J. Traina, and J. M. Bioham, *Clays Clay Miner.* **40** (4), 397 (1992).
- [52] J. Bujdak, *Appl. Clay Sci.* **34**, 58 (2006).
- [53] A. S. Sharma, and M. Ilanchelian, *Photochem. Photobiol. Sci.* **13** (12), 1741 (2014). doi:10.1039/C4PP00223G
- [54] R. H. A. Ras *et al.*, *Phys. Chem. Chem. Phys.* **9** (8), 918 (2007). doi:10.1039/b610698f
- [55] E. Okamura, J. Umemura, and T. Takenaka, *Biochim Biophys Acta Biomembr.* **1025**, 94 (1990).
- [56] M. S. Bakshi *et al.*, *J. Phys. Chem. C.* **111** (16), 5932 (2007). doi:10.1021/jp070759y